

# A Novel Combined DTC Method and SFOC System for Three-phase Induction Machine Drives with PWM Switching Method

H. Dahmardeh<sup>1</sup>, M. Ghanbari<sup>1\*</sup>, S.M. Rakhtala<sup>2</sup>

<sup>1</sup>Department of Electrical Engineering, Gorgan Branch, Islamic Azad University, Gorgan, Iran.

<sup>2</sup>Electrical Engineering Department, Golestan University, Gorgan, Iran.

**Abstract-** In this paper, a novel combined Direct Torque Control (DTC) method and Stator-Flux Oriented Control (SFOC) system to increase general performances of Three-Phase Induction Motor (TPIM) drives is proposed. The introduced control scheme includes merits of DTC for instance simple structure, less dependent on PI controller coefficients, fast dynamics, and merits of SFOC such as high precision and constant switching frequency. Specifically, the proposed control scheme includes a table-based variable structure developed on DTC strategy and a PI controller in connection with a Pulse Width Modulation (PWM) algorithm based on SFOC strategy. To confirm the usefulness of the introduced controller, simulation studies are accomplished for a 2.5kW TPIM in different situations. Results under the presented control system approve the good performances of this technique in comparison with classic DTC and classic SFOC. Investigation in TPIM performances under the introduced control system indicates relatively quick dynamic responses with low torque and stator flux ripples.

**Keyword**—AC drives, Combined DTC and SFOC, Fast dynamic response, Low torque and flux ripples, Three-phase induction motor.

## 1. INTRODUCTION

Three-Phase Induction Motor (TPIM) has very extensive range of applications in industries due to the low price, simple construction, ruggedness and high dependability [1, 2]. For high performance control of TPIMs, adjustable speed drives are normally used. Field-Oriented Control (FOC) introduced in 1972 and Direct Torque Control (DTC) introduced in 1984 are two common types of controlling techniques which are applied for TPIM drives. These methods are matured for industrial applications and offer very good dynamic characteristics and increase the performances of AC drives [3–5].

In general, the classic FOC method in comparison with the classic DTC method is more accurate in terms of speed, torque and flux ripples. Moreover, the classic FOC method uses a constant switching frequency. Although the classic DTC is not precise as much as the classic FOC, this method has some merits such as no need to coordinate transformations, it is not sensitive to the rotor resistance parameter, and implementation of this method is easy. Recently, some advanced FOC schemes in order to improve performances of electric machines such as Maximum Torque Per Ampere (MTPA) [6], operation in field weakening region [7], FOC with fuzzy logic [8], FOC with sliding mode controllers [9], and etc. have been presented. In literature, some advanced DTC schemes have also been proposed to increase the TPIM drive system performances such as Space Vector Modulation DTC (SVM-DTC) [10], predictive DTC [11], DTC with intelligent controllers [12], etc.

As alternative methods for electric machines, combined control techniques, using combined merits of DTC strategies and FOC techniques have been presented for electrical drive systems [13–21].

The aim of these methods is to obtain fast machine dynamics and smooth machine performances. Actually, combined control systems enjoy the advantages of DTC such as fast dynamics and simple structure and FOC advantages such as high steady-state precision and constant switching frequency. The combined control methods can be used for many industrial applications which need high accuracy and fast dynamics such as ABS systems.

In recent years, combined control techniques have attracted many considerations by researchers. In [13], a combined control method for doubly fed induction generators was proposed. In this study, a combined vector control method and direct power control strategy was presented. Actually, a control system based on the DTC with suitable voltage vectors was used for doubly fed induction generators. However, this method suffers from a variable switching frequency. In [14], a combined DTC technique and FOC system was proposed for linear induction motors. The suggested controller in [14] has fast dynamics and smooth performances compared to the FOC and DTC, respectively. In this paper also, the end effect in the linear induction motor was taken into consideration. As this control system was ended with the DTC, it suffers from a variable switching frequency. In [15–17], some combined control methods for synchronous motors have been presented. These methods also suffer from an inconstant switching frequency.

Besides these control techniques some combined control strategies have been developed in the literature for TPIM drives. In [18], a combined FOC strategy and DTC method for TPIM drive systems has been presented. In this paper, the derivatives of stator currents are generated using the rotor FOC strategy. Then, the derivatives of stator currents with hysteresis comparators and a switching table system are used for the inverter feeding. In [19], an improved combined control strategy for TPIM drives has been introduced. In this paper, the optimized values of voltage vectors are determined using fuzzy logic controller rules. Using the fuzzy logic controller, the selection of voltage vector was optimized and speed and torque are controlled effectively with low fluctuations and good performances. In [20], an efficiency improved sensorless combined control system based on extended kalman filter with a field weakening algorithm for TPIM drives has been proposed.

Received: 22 Oct. 2021

Revised: 27 Nov. 2021

Accepted: 03 Dec. 2021

\*Corresponding author: E-mail: ghanbari@gorganiau.ac.ir (M. Ghanbari)

DOI:10.22098/joape.2023.9717.1679

**Research Paper**

©2023 University of Mohaghegh Ardabili. All rights reserved

In aforementioned strategies, the control system starts with FOC system and finishes with DTC method. Due to using switching table strategy, these methods suffer from a variable switching frequency. In [21], a developed combined DTC system and FOC approach for TPIM drives was proposed to enhance TPIM drive system performances in which a five-level inverter with SVM switching method has been used. The suggested control system in [21] contains the advantages of DTC and FOC schemes. This method suffers from tuning of PI controller coefficients, complex structure, and dependency to variation of machine parameters. Another control method which is presented for TPIM drives is Model Predictive Control (MPC) methods [22–25]. In [22], to decrease the torque fluctuation in DTC of TPIM drives a MPC-based DTC technique for a direct matrix converter fed TPIM using two novel look-up tables was presented. In [23], a passivity-based MPC method for three-level neutral point clamped inverter to improve the robustness and reduce the computational burden was proposed for TPIM drives. A cascaded MPC method was proposed in [24] for TPIM drives that avoided weighting factors. In [25], a speed encoderless MPC control using six switching states of the matrix converter that generate zero common mode voltage was proposed for TPIM drives. Commonly, MPC techniques have simple structure and good performances. Nevertheless, these strategies have some drawbacks for example high sampling frequency, variable switching frequency, weighting factor optimization, etc.

In this study, a novel combined DTC strategy and Stator FOC (SFOC) system is introduced for TPIM drives. This composed controller utilizes the advantages of both DTC and SFOC methods. In particular, the proposed control scheme contains a developed switching table approach in connection with a SFOC system based on Pulse Width Modulation (PWM) switching strategy. Different from previous studies, the composed controller is modelled on DTC strategy as a control law, and those of SFOC technique as a modulation method. So that a table-based variable structure approach is presented in cooperation with a PI controller. In this study, different simulations approve that the machine performances under the presented composed controller is better than the one under classic DTC and classic SFOC methods in terms of  $|\lambda_s|$  and  $T_e$  responses. The main contributions of this study are:

- A combined control technique is introduced based on a modified switching-table DTC method in connection with a PI controller and PWM.
- Compared to the prior combined control techniques for example [18–20], in the suggested control method the control law is according to DTC and the modulation is according to VC. It means that the variable switching frequency which is the main drawbacks of the prior combined control techniques is rectified by the suggested control method.
- The suggested combined control strategy in this study has better dynamics owing to fewer PI controllers and lower complexity compared to [21].

The work continues in Section 2 by (d-q) model of TPIMs. In Sections 3 and 4, classic SFOC and classic DTC strategies have been presented, respectively. The proposed combined control system is presented in Section 5. In Section 6, several simulations are presented to evaluate the TPIM drive under the introduced control system based on MATLAB/Simulink software. Finally, Section 7 provides some concluding remarks.

## 2. (D-Q) MODEL OF A TPIM

The TPIM model in the stationary coordinate (superscript “s”) can be expressed by (1)–(10) [26]:

$$v_{ds}^s = r_s i_{ds}^s + l_s p i_{ds}^s + l_m p i_{dr}^s \quad (1)$$

$$v_{qs}^s = r_s i_{qs}^s + l_s p i_{qs}^s + l_m p i_{qr}^s \quad (2)$$

$$v_{dr}^s = 0 = l_m p i_{qs}^s - \omega_r l_m i_{ds}^s + r_r i_{qr}^s + l_r p i_{qr}^s - \omega_r l_r i_{dr}^s \quad (3)$$

$$v_{dr}^s = 0 = l_m p i_{qs}^s - \omega_r l_m i_{ds}^s + r_r i_{qr}^s + l_r p i_{qr}^s - \omega_r l_r i_{dr}^s \quad (4)$$

$$\lambda_{ds}^s = l_s i_{ds}^s + l_m i_{dr}^s \quad (5)$$

$$\lambda_{qs}^s = l_s i_{qs}^s + l_m i_{qr}^s \quad (6)$$

$$\lambda_{dr}^s = l_m i_{ds}^s + l_r i_{dr}^s \quad (7)$$

$$\lambda_{qr}^s = l_m i_{qs}^s + l_r i_{qr}^s \quad (8)$$

$$T_e = N_p (l_m i_{qs}^s i_{dr}^s - l_m i_{ds}^s i_{qr}^s) \quad (9)$$

$$T_e - T_l = 1/N_p (J p \omega_r + F \omega_r) \quad (10)$$

where,  $v_{ds,qs,dr,qr}^s$  are the stator and rotor voltages.  $i_{ds,qs,dr,qr}^s$  are the stator and rotor currents.  $\lambda_{ds,qs,dr,qr}^s$  are the stator and rotor fluxes.  $p$  is the differential operator.  $l_{s,r,m}$  denote the stator, rotor self and mutual inductances.  $r_{s,r}$  are the stator and rotor resistances.  $\omega_r$  is the machine speed.  $T_{e,l}$  are electromagnetic and load torques.  $N_p, J$  are the number of pole pairs and moment of inertia.

## 3. CLASSIC SFOC STRATEGY FOR A TPIM

In the SFOC system, the machine equations should be written in the rotating coordinate. Besides, the stator flux vector should be constant and aligned with d-axis, which means:  $\lambda_{ds} = |\lambda_s|$  and  $\lambda_{qs} = 0$ . As a result, the dynamic SFOC model of a TPIM can be expressed by (11)–(16) [27]:

$$|\lambda_s| = l_s \left( \frac{1 + \sigma \tau_r p}{1 + \tau_r p} \right) i_{ds} - \left( \frac{\sigma \tau_r l_s \omega_{sl}}{1 + \tau_r p} \right) i_{qs} \quad (11)$$

$$T_e = N_p |\lambda_s| i_{qs} \quad (12)$$

$$\omega_{sl} = \frac{l_s}{\tau_r} \left( \frac{1 + \sigma \tau_r p}{|\lambda_s| - \sigma l_s i_{ds}} \right) i_{qs} \quad (13)$$

$$\theta_e = \int (\omega_{sl} + \omega_r) dt \quad (14)$$

$$v_{ds} = \frac{r_s (\tau_s + \tau_r)}{\tau_r} \left( 1 + \frac{\sigma \tau_s \tau_r}{\tau_s + \tau_r} p \right) i_{ds} - \sigma l_s \omega_{sl} i_{qs} - \frac{|\lambda_s|}{\tau_r} \quad (15)$$

$$v_{qs} = \frac{r_s (\tau_s + \tau_r)}{\tau_r} \left( 1 + \frac{\sigma \tau_s \tau_r}{\tau_s + \tau_r} p \right) i_{qs} + \sigma l_s \omega_{sl} i_{ds} + \omega_r |\lambda_s| \quad (16)$$

where,

$$\sigma = 1 - \left( \frac{l_m^2}{l_s l_r} \right), \quad \tau_r = \frac{l_r}{r_r}, \quad \tau_s = \frac{l_s}{r_s} \quad (17)$$

Using (11)–(17), the structure of the classic SFOC system in the torque control mode can be shown as Fig. 1.

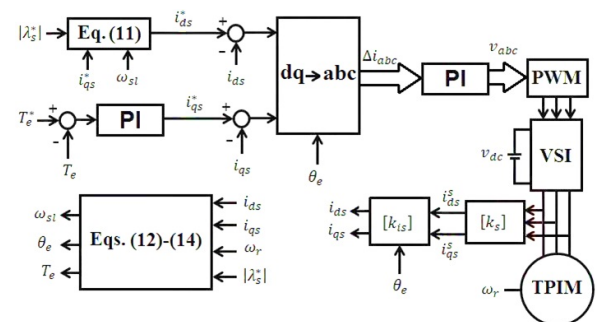


Fig. 1: Structure of the classic SFOC system in the torque control mode

In Fig. 1, the stator voltages are generated using two PI controllers. In this figure,  $i_{ds}^*$  and  $i_{qs}^*$  indicate reference stator currents in the rotating coordinate and they are achieved from (11) and a PI controller, respectively. Furthermore, the flux position, torque, and slip speed are achieved based on (12)-(14). Additionally, blocks  $[k_{is}]$  and  $[k_{vs}]$  are transformation matrices to transform the stator currents and voltages from the stationary coordinate to the rotating coordinate. Besides, the block  $[k_s]$  is a transformation matrix to transform the stator quantities from (a-b-c) coordinate to the (d-q) stationary coordinate.

#### 4. CLASSIC DTC STRATEGY FOR A TPIM

The classic DTC strategy based on switching table was initially introduced in [28]. In this method, the  $|\lambda_s|$  and  $T_e$  are controlled directly without using current controllers. The principles of the classic DTC method for TPIM drives can be explained by the torque and stator flux equations as (18)-(22) [29]:

$$\lambda_{ds}^s = \int (v_{ds}^s - r_s i_{ds}^s) dt \quad (18)$$

$$\lambda_{qs}^s = \int (v_{qs}^s - r_s i_{qs}^s) dt \quad (19)$$

$$|\lambda_s| = \sqrt{\lambda_{ds}^s{}^2 + \lambda_{qs}^s{}^2} \quad (20)$$

$$\theta_s = \tan^{-1} \left( \frac{\lambda_{qs}^s}{\lambda_{ds}^s} \right) \quad (21)$$

$$T_e = \frac{N_p l_m}{\sigma l_s l_r} |\lambda_s| |\lambda_r| \sin \delta \quad (22)$$

where,  $\delta$  is the stator flux angle. Using (18)-(22), the structure of the classic DTC can be displayed as Fig. 2. As shown in this figure, the decouple control of the  $T_e$  and  $|\lambda_s|$  is done by the three-level hysteresis comparator and two-level hysteresis comparator, respectively [29]. In Fig. 2, the selection of switching

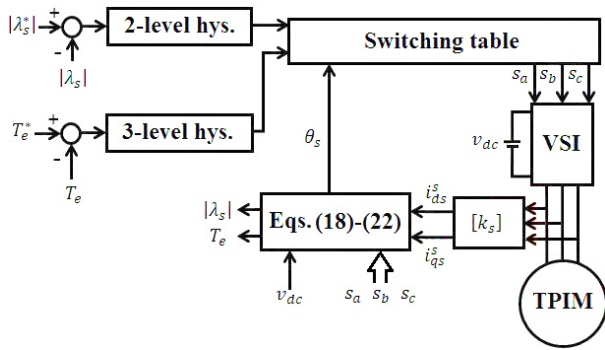


Fig. 2: Structure of the classic DTC strategy

states is obtained from the switching table presented in Table 1 [29]. The voltage vectors in the switching table are determined based on increasing or decreasing of the torque and stator flux.

#### 5. PROPOSED COMBINED DTC METHOD AND SFOC SYSTEM FOR A TPIM WITH PWM SWITCHING METHOD

SFOC and DTC are two common control methods which are used for TPIM drives. These two strategies have some important characteristics which are compared in Table 2.

It is important to note that despite various differences between the SFOC and DTC, these control strategies enjoy a common foundation. In this section, the proposed combined control system

for a TPIM drive with PWM switching method is presented. Based on the SFOC strategy, we can write:

$$\Delta |\lambda_s| \propto \Delta i_{ds} \quad (23)$$

$$\Delta T_e \propto \Delta i_{qs} \quad (24)$$

where,  $\Delta$  stands for very small variations. Based on (22), the variation of the torque is proportional to the variation of the  $\delta$  [18]:

$$\Delta T_e \propto \Delta \delta \quad (25)$$

In addition, based on the SFOC principals,

$$\Delta |\lambda_s| \cong \Delta \lambda_{ds} \quad (26)$$

Based on the classic SFOC strategy, the stator and rotor flux vectors can be displayed as Fig. 3. By assuming small variations of  $\Delta \delta$  in

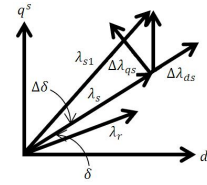


Fig. 3: Structure of the classic DTC strategy

Fig. 3,  $\sin \Delta \delta$  is achieved as:

$$\sin \Delta \delta \cong \frac{\Delta \lambda_{qs}}{|\lambda_s|} \rightarrow \Delta \delta \propto \Delta \lambda_{qs} \quad (27)$$

and so:

$$\Delta T_e \propto \Delta \lambda_{qs} \quad (28)$$

Based on the classic DTC strategy (equations (18) and (19)), with a good approximation, the stator flux variation can be written as (29):

$$\begin{cases} \Delta \lambda_{ds}^s \approx v_{ds}^s \cdot \Delta t \\ \Delta \lambda_{qs}^s \approx v_{qs}^s \cdot \Delta t \end{cases} \quad (29)$$

Equation (29) result in,

$$\begin{cases} \Delta \lambda_{ds}^s \propto v_{ds}^s \rightarrow v_{abc} \propto \Delta \lambda_{abc} \\ \Delta \lambda_{qs}^s \propto v_{qs}^s \end{cases} \quad (30)$$

It is notable that the DTC switching table is calculated based on (25)-(30).

By using (23), (24), (26), and (28), it can be found that:

$$\begin{cases} \Delta i_{ds} \propto \Delta \lambda_{ds} \\ \Delta i_{qs} \propto \Delta \lambda_{qs} \end{cases} \rightarrow \begin{cases} \Delta i_{ds}^s \propto \Delta \lambda_{ds}^s \\ \Delta i_{qs}^s \propto \Delta \lambda_{qs}^s \end{cases} \rightarrow \Delta i_{abc} \propto \Delta \lambda_{abc} \quad (31)$$

Equation (31) shows that using the control equations based on SFOC strategy, the stator flux variation is related to the stator current variation. Also, equation (30) indicates that based on DTC equations, the stator flux variation is related to the machine voltage. As a result, there is a direct relationship between the machine voltage, stator flux variation, and stator current variation as (32):

$$v_{abc} \propto \Delta \lambda_{abc} \propto \Delta i_{abc} \quad (32)$$

Using this fact, the produced voltages of DTC system are aligned with the stator current variations. Based on the SFOC system, the  $\Delta i_{abc}$  using PI controllers can create the machine voltages as (33) [30]:

$$v_{abc}^* = \left( K_p + \frac{K_i}{s} \right) \Delta i_{abc}^* \quad (33)$$

where,  $K_p, K_i$  are proportional and integral coefficients, respectively. These voltages as given in (33) using PWM can be applied to the inverter. As can be seen from (30) and (31), the stator flux deviation is defined as a common base between

Table 1: Classic switching table

$\lambda_s^h$	$T_e^h$	Sector					
		1	2	3	4	5	6
-1	+1	010 ( $V_3$ )	011 ( $V_4$ )	001 ( $V_5$ )	101 ( $V_6$ )	100 ( $V_1$ )	110 ( $V_2$ )
	0	111 ( $V_7$ )	000 ( $V_0$ )	111 ( $V_7$ )	000 ( $V_0$ )	111 ( $V_7$ )	000 ( $V_0$ )
	-1	001 ( $V_5$ )	101 ( $V_6$ )	100 ( $V_1$ )	110 ( $V_2$ )	010 ( $V_3$ )	011 ( $V_4$ )
+1	+1	110 ( $V_2$ )	010 ( $V_3$ )	011 ( $V_4$ )	001 ( $V_5$ )	101 ( $V_6$ )	100 ( $V_1$ )
	0	000 ( $V_0$ )	111 ( $V_7$ )	000 ( $V_0$ )	111 ( $V_7$ )	000 ( $V_0$ )	111 ( $V_7$ )
	-1	101 ( $V_6$ )	100 ( $V_1$ )	110 ( $V_2$ )	010 ( $V_3$ )	011 ( $V_4$ )	001 ( $V_5$ )

Table 2: Comparison between the SFOC and DTC

Items	Strategies	
	SFOC	DTC
Torque ripples	Low	High
Dynamic response	Slow	Fast
Switching frequency	Constant	Variable
Difficulty	High	Low

Table 3: Combined control switching table

$\lambda_s^h$	$T_e^h$	Sector					
		1	2	3	4	5	6
-1	+1	$\Delta i_3$	$\Delta i_4$	$\Delta i_5$	$\Delta i_6$	$\Delta i_1$	$\Delta i_2$
	0	$\Delta i_7$	$\Delta i_0$	$\Delta i_7$	$\Delta i_0$	$\Delta i_7$	$\Delta i_0$
	-1	$\Delta i_5$	$\Delta i_6$	$\Delta i_1$	$\Delta i_2$	$\Delta i_3$	$\Delta i_4$
+1	+1	$\Delta i_2$	$\Delta i_3$	$\Delta i_4$	$\Delta i_5$	$\Delta i_6$	$\Delta i_1$
	0	$\Delta i_0$	$\Delta i_7$	$\Delta i_0$	$\Delta i_7$	$\Delta i_0$	$\Delta i_7$
	-1	$\Delta i_6$	$\Delta i_1$	$\Delta i_2$	$\Delta i_3$	$\Delta i_4$	$\Delta i_5$

DTC and SFOC methods. Based on this, a combined DTC method and SFOC technique is presented so that it employs DTC control structure to generate control signals, and those of SFOC to apply the signals to the inverter. The recommended composed controller not only preserves the control structure as simple as DTC, but also provides a switching algorithm as SFOC. In other words, although the composed controller abstains from the oriented reference coordinates, it is equipped with the simple PWM switching algorithm. Hence, the proposed composed control system enjoys less dependency on parameters of controllers and machine, fast dynamics, and low  $|\lambda_s|$  and  $T_e$  ripples, in comparison with SFOC and DTC, respectively. Based on Table 1 and (32), the combined control switching table can be shown as Table 3. Finally, using Fig. 1, Fig. 2, Table 2, (32), and (33), the structure of the proposed combined control system can be shown as Fig 4.

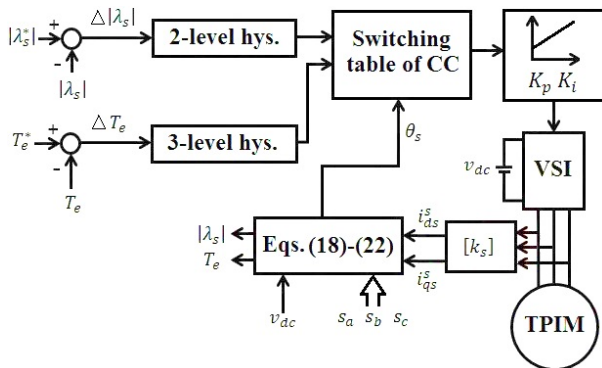


Fig. 4: Structure of the proposed combined control system

As a sample of the current deviation selection, if  $\Delta T_e = +1$ ,  $\Delta \lambda_s = -1$  and the angle is between  $(-\pi)/6$  and  $\pi/6$  then based on Tables 1 and 3,  $\Delta i_3$  or  $010(V_3)$  is chosen as the PI controller input. After selection of  $\Delta i_3$  or  $010(V_3)$ ,  $V_{abc}$  can be determined. As can be seen from Fig. 4, the composed controller expands DTC control rule in cooperation with

those of SFOC in such way that employs control merits of DTC and switching merits of SFOC together. To compare the proposed composed controller with the classic SFOC, unlike the SFOC system that suffers from PI tunings and low dynamic responses, the composed controller enjoys a more simple structure with fast dynamics by employing a table-based variable structure imbedded to a PI controller. In addition, the composed controller outweighs the classic DTC in terms of low  $|\lambda_s|$  and  $T_e$  ripples, and uniform switching. It is notable that the PWM switching approach is used in the proposed combined control structure. Using the PWM algorithm instead of the switching table leads to lower harmonics and switching losses as well as lower audio noises. Nevertheless, using the PWM increases the calculation burden and system complexities.

## 6. SIMULATION RESULTS AND COMPARISONS

To confirm the performances of the introduced combined DTC method and SFOC system, the TPIM drive under the proposed control system is simulated using MATLAB/Simulink software at different situations. Besides, in order to compare the proposed technique with classic DTC strategy and classic SFOC strategy, these methods are also simulated. The proposed method, classic DTC strategy, and classic SFOC strategy are simulated based on Fig. 4, Fig. 2, and Fig.1, respectively. The coefficients of PI controllers are accomplished using the method presented in [31] for all simulations. For simulations, three scenarios are considered under MTPA. The TPIM specifications are given in Table 4.

### Scenario 1:

Fig. 5 shows the comparison of the classic SFOC strategy, classic DTC strategy, and proposed method. Fig. 5(a) shows the results of the  $|\lambda_s|$  and  $T_e$  responses of the classic SFOC strategy. Fig. 5(b) shows the results of the  $|\lambda_s|$  and  $T_e$  responses of the classic DTC strategy. Fig. 5(c) shows the results of the  $|\lambda_s|$  and  $T_e$  responses of the proposed method. For this scenario, the torque reference changes from 1Nm to 3Nm at  $t=0.1s$ . Also, the stator flux reference changes from 0.4Wb to 0.5Wb at  $t=0.1s$ . In Fig.5, a simple MPTA table-based strategy [32] has been employed to simultaneously investigate torque and flux control responses.

Fig. 5 shows that using the classic SFOC strategy, classic DTC strategy, and proposed combined control technique, the real  $|\lambda_s|$  and  $T_e$  signals during different torque and stator flux references can follow their reference values suitably without any significant overshoot and steady-state errors. The comparison between the classic DTC strategy and proposed composed technique shows that the classic DTC strategy is more appropriate in terms of fast dynamics. However, using the proposed combined control system low ripples in both  $|\lambda_s|$  and  $T_e$  responses can be obtained. Moreover, the comparison between the classic SFOC strategy and proposed composed technique indicates that the classic SFOC strategy is more desirable in terms of  $|\lambda_s|$  and  $T_e$  ripples. Nevertheless, using the proposed combined control strategy, a fast dynamic response in both torque and stator flux can be achieved.

Based on the simulation results of Fig. 5, the peak to peak  $|\lambda_s|$  and  $T_e$  ripples using the classic SFOC strategy are about 0.00098Wb and 0.051Nm, respectively. The peak to peak  $|\lambda_s|$  and  $T_e$  ripples using the classic DTC strategy are about 0.0052Wb and 0.31Nm, respectively. Finally, the peak to peak  $|\lambda_s|$  and  $T_e$  ripples

Table 4: TPIM specifications

$P_{rated}$	$V_{rated}$	$f_{rated}$	$\omega_{rrated}$	$N_p$	$r_s$	$r_r$	$l_{s,r}$	$l_m$
2.5kW	220V	50Hz	1420rpm	2	3.67 $\Omega$	1.82 $\Omega$	0.315H	0.303H

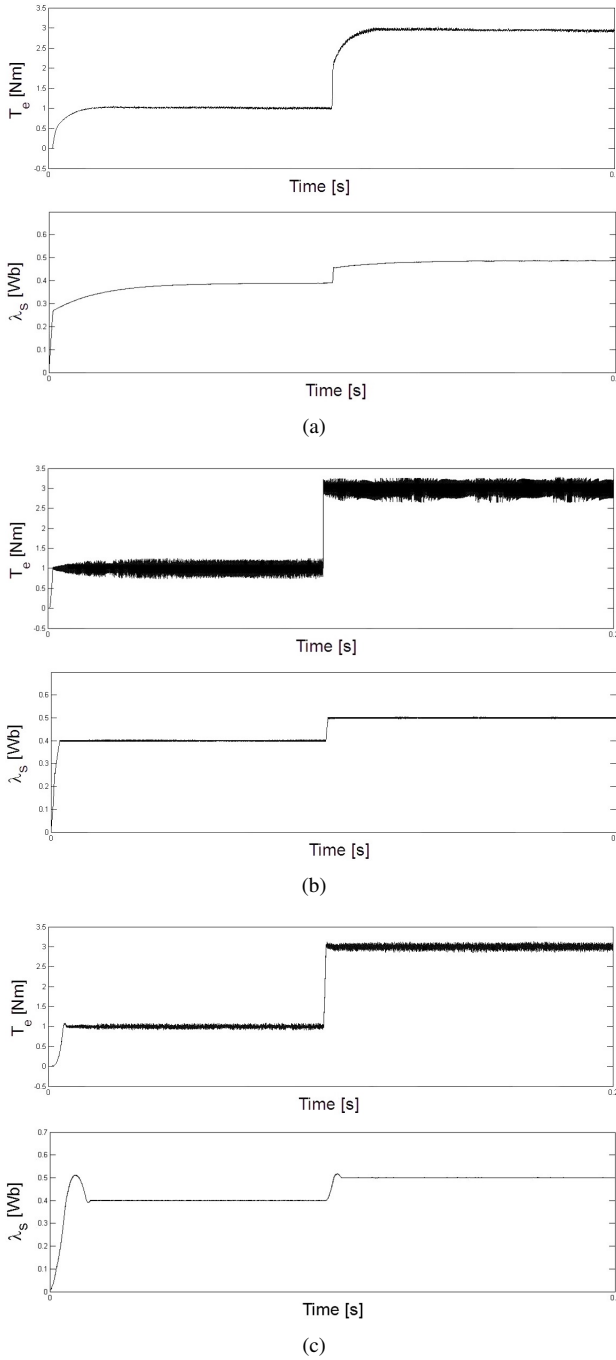


Fig. 5: Comparison of the classic SFOC strategy, classic DTC strategy, and proposed method for the scenario 1; (a) classic SFOC strategy, (b) classic DTC strategy, (c) proposed method

using the proposed composed strategy are about 0.0029Wb and 0.105Nm, respectively. Furthermore, based on the torque responses of Fig. 5, the time to reach steady-state from 1Nm to 3Nm using the classic SFOC strategy, classic DTC strategy, and proposed composed control strategy are 5ms, 1ms, and 1.5ms, respectively. To sum up, Table 5 represents a comparison of SFOC, DTC, and suggested combined control strategies for the scenario 6.

Table 5: Comparison of SFOC, DTC, and suggested combined control strategies for the scenario 1

Items	Strategies		
	SFOC	DTC	Combined control
Torque ripple	0.051Nm	0.31Nm	0.105Nm
Flux ripple	0.00098Wb	0.0052Wb	0.0029Wb
Torque dynamic response ( $T_e^*$ : 1Nm $\rightarrow$ 3Nm)	5ms	1ms	1.5ms

Table 6: Comparison of SFOC, DTC, and suggested combined control strategies for the scenario 2

Items	Strategies		
	SFOC	DTC	Combined control
Torque ripple	0.05Nm	0.3Nm	0.1Nm
Flux ripple	0.0009Wb	0.0057Wb	0.003Wb
Torque dynamic response ( $T_e^*$ : 1Nm $\rightarrow$ 3Nm)	12ms	2.5ms	4ms

### Scenario 2:

Fig. 6 shows the results of the  $|\lambda_s|$  and  $T_e$  responses under the classic SFOC strategy (Fig. 6(a)), classic DTC strategy (Fig. 6(b)), and proposed method (Fig. 6(c)). For this scenario, the torque reference changes from -3Nm to 3Nm at  $t=0.025s$ . Also, the stator flux reference is set to 0.55Wb.

It is clear that the three  $T_e$  signals and three  $|\lambda_s|$  signals are totally similar except for nearly more fluctuations for the classic DTC and nearly less fluctuations for the classic SFOC. These figures also approve that the  $|\lambda_s|$  and  $T_e$  responses under the introduced composed control technique based on the PWM is slower than that gained under the classic DTC technique; but faster than that obtained under the classic SFOC.

Based on Fig. 6, the torque ripple using the classic SFOC strategy, classic DTC strategy, and proposed composed strategy are almost 0.05Nm, 0.3Nm, and 0.1Nm, respectively. Additionally, based on the torque responses of Fig. 6, the time from -3Nm to 3Nm using the classic SFOC strategy, classic DTC strategy, and proposed strategy are 12ms, 2.5ms and 4ms, respectively.

To sum up, Table 6 represents a comparison of SFOC, DTC, and suggested combined control strategies for the scenario 2. The results of Fig. 5 and Fig. 6 show that the drive system performances under the introduced control technique combines the good features of the classic DTC and classic SFOC strategies. Fig. 5 and Fig. 6 indicate that the introduced control system in this paper can provide high dynamic performances and low  $|\lambda_s|$  and  $T_e$  ripples for the TPIM drive system and can be used to control drive systems in demanding industrial applications.

### Scenario 3:

Fig. 7 shows the simulation results of the proposed combined control method in the speed control condition. In Fig. 7, the TPIM is driven by the speed of 150rad/s and flux linkage of 0.55Wb. In this figure, a step load torque of 1Nm is applied at  $t=15s$ .

Fig. 7 demonstrates that the real speed under the suggested combined control technique tracks its reference without any substantial error. According to the results, a fast dynamic torque with low ripple is obtained. Additionally, the stator flux linkage tracks its reference value precisely during no-load and load states. To sum up, Table 7 represents a comparison of SFOC, DTC, and suggested combined control strategies.

## 7. CONCLUSION

A composed DTC method and SFOC strategy for TPIM drives with PWM switching method based on selective features of these

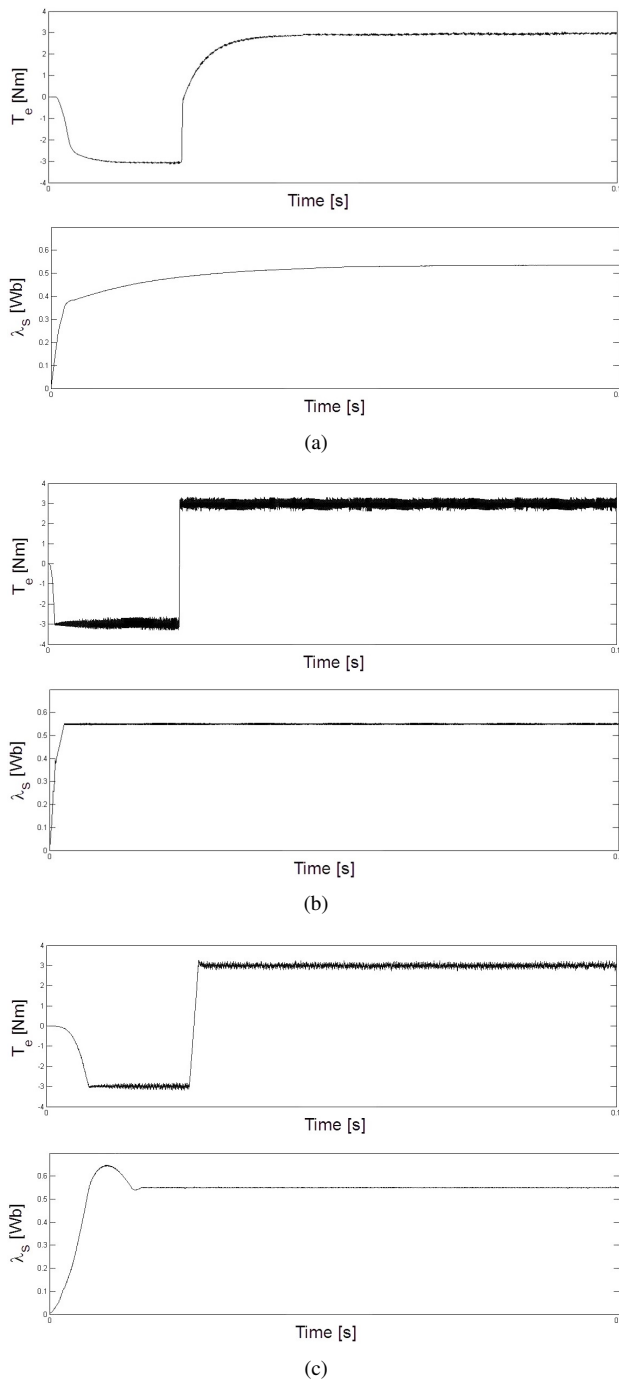


Fig. 6: Comparison of the classic SFOC strategy, the classic DTC strategy, and the proposed method for the scenario 2; (a) classic SFOC strategy, (b) classic DTC strategy, (c) proposed method

control techniques is proposed in this study. In fact, the proposed control system is a modified DTC strategy with a constant switching frequency. The performance of the proposed control system is compared with the classic DTC and classic SFOC schemes. The results confirm that the combined system keeps high dynamic responses like DTC strategy. Moreover, the proposed method keeps low  $|\lambda_s|$  and  $T_e$  ripples like SFOC strategy. In other words, the  $|\lambda_s|$  and  $T_e$  responses under the proposed composed control strategy are slower than that gained under the classic DTC method; but faster than that obtained under the classic SFOC method. In addition, the  $|\lambda_s|$  and  $T_e$  ripples according to the proposed composed control strategy are less than the  $|\lambda_s|$  and  $T_e$  ripples based on the classic

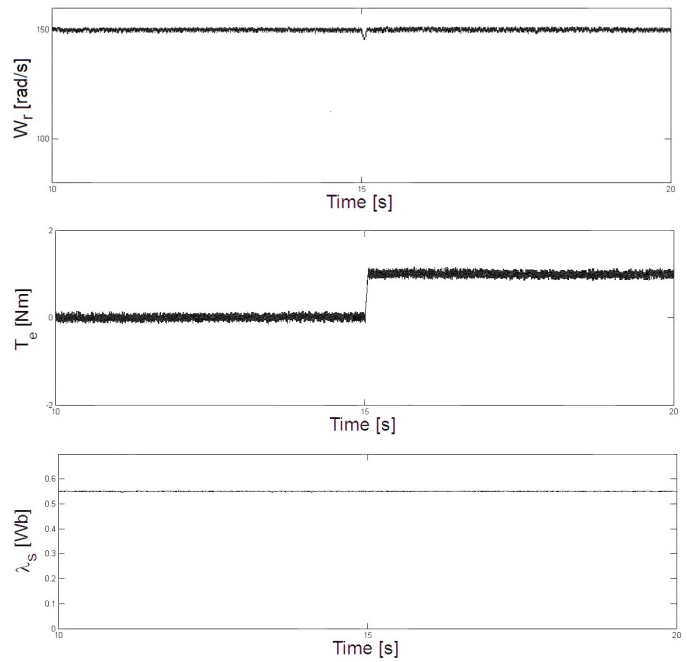


Fig. 7: Simulation results of the proposed combined control method in the speed control condition

Table. 7: Comparison of SFOC, DTC, and suggested combined control strategies

	SFOC	DTC	Combined control
Frame transformations	Need	No need	No need
Reference frame	Rotating	Stationary	Stationary
Current control	Need	No need	Need
PWM	Need	No need	Need
Switching frequency	Constant	Variable	Constant
Complexity	High	Low	Low
Controller type	PI	Hysteresis	PI

DTC method; but more than the  $|\lambda_s|$  and  $T_e$  ripples based on the classic SFOC method.

## REFERENCES

- [1] A. Gholipour, et al., "Sensorless FOC Strategy for Current Sensor Faults in Three-Phase Induction Motor Drives," *J. Oper. Autom. Power Eng.*, 2021.
- [2] M. Nikpayam, et al., "Vector Control Methods for Star-Connected Three-Phase Induction Motor Drives Under the Open-Phase Failure," *J. Oper. Autom. Power Eng.*, 2021.
- [3] M. Wolkiewicz, et al., "Online stator inter-turn short circuits monitoring in the DFOC induction-motor drive," *IEEE Trans. Ind. Electron.*, vol. 63, pp. 2517-2528, Jan 2016.
- [4] M. Jannati, et al., "A new speed sensorless SVM-DTC in induction motor by using EKF," in *2013 IEEE Student Conf. on Research and Development*, 2013, pp. 94-99.
- [5] M. Jannati, et al., "Novel Method of FOC to Speed Control in Three-Phase IM under Normal and Faulty Conditions," *Int. J. of Power Elec. and Drive Syst.*, vol. 6, pp. 831-841, Dec 2015.
- [6] T. Sun, et al., "Integration of FOC with DFVC for interior permanent magnet synchronous machine drives," *IEEE Access*, vol. 8, pp. 97935-97945, May 2020.
- [7] Q. Shen, et al., "An Improved Field Weakening Control of IPMSM with Fuzzy Anti-Windup Strategy," in *2021 IEEE 4th Int. Elec. and Energy Conf.*, 2021, pp. 1-6.
- [8] M. A. Hannan, et al., "Optimization techniques to enhance the performance of induction motor drives: A review," *Renew. Sustain. Energy Rev.*, vol. 81, pp. 1611-1626, Jan 2017.

- [9] X. Liu, et al., "Combined Speed and Current Terminal Sliding Mode Control with Nonlinear Disturbance Observer for PMSM Drive," *IEEE Access*, vol. 6, pp. 29594-29601, May 2018.
- [10] Z. Zhang, et al., "Novel direct torque control based on space vector modulation with adaptive stator flux observer for induction motors," *IEEE Trans. Magn.*, vol. 46, pp. 3133-3136, Jul 2010.
- [11] B. Cao, et al., "Direct torque model predictive control of a five-phase permanent magnet synchronous motor," *IEEE Trans. Power Electron.*, vol. 36, pp. 2346-2360, Jul 2020.
- [12] S. Inayah and A. Khedher, "Fuzzy-Self-Tuning PI Speed Regulator for DTC of Three-Level Inverter fed IM," in *2020 17<sup>th</sup> Int. Multi-Conf. on Syst., Signals & Devices*, 2020, pp. 709-714.
- [13] J. Mohammadi, et al., "A combined vector and direct power control for DFIG-based wind turbines," *IEEE Trans. Sustainable Energy*, vol. 5, pp. 767-775, Feb 2014.
- [14] H. Karimi, et al., "Combined vector and direct thrust control of linear induction motors with end effect compensation," *IEEE Trans. Energy Convers.*, vol. 31, pp. 196-205, Oct 2016.
- [15] S. Vaez-Zadeh and E. Daryabeigi, "Combined vector and direct torque control methods for IPM motor drives using emotional controller (BELBIC)," in *2011 2nd Power Elec., Drive Sys. and Tech. Conf.*, 2011, pp. 145-150.
- [16] E. Daryabeigi and S. Vaez-Zadeh, "A Combined Control for Fast and Smooth Performance of IPM Motor Drives over Wide Operating Conditions," *IEEE Transactions on Energy Convers.*, vol. 33, pp. 1384-1391, Feb 2018.
- [17] M. J. Navardi, et al., "Torque and Flux Ripples Minimization of Permanent Magnet Synchronous Motor by a Predictive-Based Hybrid Direct Torque Control," *IEEE J. Emerging Sel. Top. Power Electron.*, vol. 6, pp. 1662-1670, May 2018.
- [18] S. Vaez-Zadeh and E. Jalali, "Combined vector control and direct torque control method for high performance induction motor drives," *Energy Convers. Manage.*, vol. 48, pp. 3095-3101, Dec 2007.
- [19] Z. Boulghasoul, et al., "Intelligent control for torque ripple minimization in combined vector and direct controls for high performance of IM drive," *J. Electr. Eng. Technol.*, vol. 7, pp. 546-557, Jul 2012.
- [20] M. Farasat, et al., "Efficiency improved sensorless control scheme for electric vehicle induction motors," *IET Electr. Syst. Transp.*, vol. 4, pp. 122-131, Aug 2014.
- [21] H. M. Suryawanshi, et al., "Modified combined dtc and foc based control for medium voltage induction motor drive in svm controlled dcml," *EPE J.*, vol. 23, pp. 23-32, Dec 2013.
- [22] H. Dan, et al., "Model predictive control-based direct torque control for matrix converter-fed induction motor with reduced torque ripple," *CES Trans. Electr. Mach. Syst.*, vol. 5, pp. 90-99, Jul 2021.
- [23] F. Wang, et al., "Passivity-based model predictive control of three-level inverter-fed induction motor," *IEEE Trans. Power Electron.*, vol. 36, pp. 1984-1993, Jul 2020.
- [24] N. S. P. Musunuru and S. Srirama, "Cascaded Predictive Control of a Single Power Supply-Driven Four-Level Open-End Winding Induction Motor Drive Without Weighting Factors," *IEEE J. Emerging Sel. Top. Power Electron.*, vol. 9, pp. 2858-2867, Aug 2020.
- [25] T. N. Mir, et al., "FS-MPC-Based Speed Sensorless Control of Matrix Converter Fed Induction Motor Drive With Zero Common Mode Voltage," *IEEE Trans. Ind. Electron.*, vol. 68, pp. 9185-9195, Sep 2020.
- [26] M. Jannati, et al., "Performance Evaluation of the Field-Oriented Control of Star-Connected 3-Phase Induction Motor Drives under Stator Winding Open-Circuit Faults," *J. Power Electron.*, vol. 16, pp. 982-993, May 2016.
- [27] M. Boussak and K. Jarray, "A high-performance sensorless indirect stator flux orientation control of induction motor drive," *IEEE Trans. Ind. Electron.*, vol. 53, pp. 41-49, Feb 2006.
- [28] I. Takahashi and T. Noguchi, "A new quick-response and high-efficiency control strategy of an induction motor," *IEEE Trans. Ind. Appl.*, vol. 5, pp. 820-827, Sep 1986.
- [29] P. Vas, *Sensorless vector and direct torque control*, Oxford Univ. Press, 1998.
- [30] C. Lascu, et al., "Direct torque control of sensorless induction motor drives: a sliding-mode approach," *IEEE Trans. Ind. Appl.*, vol. 40, pp. 582-590, Mar 2004.
- [31] M. Jannati, et al., "A simple vector control technique for 3-phase induction motor under open-phase fault based on GA for tuning of speed PI controller," in *2014 IEEE Conf. on Energy Convers.*, 2014, pp. 213-218.
- [32] S. Bolognani, et al., "Online MTPA control strategy for DTC synchronous-reluctance-motor drives," *IEEE Trans. Power Electron.*, vol. 26, pp. 20-28, Jan 2011.